

# The Hot Spots and Transition from d-Wave to Another Pairing Symmetry in the Electron-Doped Cuprate Superconductors

V. A. Khodel,<sup>1,2</sup> Victor M. Yakovenko,<sup>2</sup> M. V. Zverev,<sup>1</sup> and Haeyoung Kang<sup>3,2</sup>

<sup>1</sup>Russian Research Centre Kurchatov Institute, Moscow, 123182, Russia

<sup>2</sup>Condensed Matter Theory Center and Center for Superconductivity Research,

Department of Physics, University of Maryland, College Park, Maryland 20742-4111, USA

<sup>3</sup>Department of Physics, Ewha Womans University, Seoul 120-750, South Korea

(Dated: cond-mat/0307454, 17 July 2003)

We present a simple theoretical explanation for a transition from d-wave to another superconducting pairing observed in the electron-doped cuprates. The  $d_{x^2-y^2}$  pairing potential, which has the maximum magnitude and opposite signs at the hot spots on the Fermi surface, becomes suppressed with the increase of electron doping, because the hot spots approach the Brillouin zone diagonals, where it vanishes. Then, the  $d_{x^2-y^2}$  pairing is replaced by either singlet s-wave or triplet p-wave pairing. We argue in favor of the latter and propose experiments to uncover it.

PACS numbers: 74.72.-h 74.20.Rp 74.20.Mn

**Introduction.** The superconducting pairing symmetry in the electron-doped cuprates, such as  $Nd_{2-x}Ce_xCuO_4$  and  $Pt_{2-x}Ce_xCuO_4$ , has been debated for a long time. Originally, it was thought to be of the s-wave type [1] and then of the d-wave type [2]. Recently, evidence was found for a transition from d-to s-wave pairing symmetry with the increase of electron doping [3, 4]. Biswas et al. [3] concluded that  $Pt_{2-x}Ce_xCuO_4$  has d-wave pairing at  $x = 0.15$  and s-wave pairing at  $x = 0.17$ . In this Letter, we propose a simple scenario for the transition from the d-wave to another pairing symmetry and argue that the latter can actually be triplet p-wave.

First we present a qualitative picture in terms of the Fermi surface geometry shown in Fig. 1. According to Ref. [5], the antiferromagnetic spin fluctuations (ASF) peaked at the wave vector  $Q = ( ; )$  are responsible for d-wave superconductivity in the hole-doped cuprates. The interaction via ASF has the highest strength at the so-called hot spots, the points on the Fermi surface connected to each other by the vector  $Q$ . These points are labeled in Fig. 1 by the consecutive numbers from 1 to 8. Since the interaction via ASF is repulsive in the singlet channel, the superconducting pairing potential ( $\rho$ ) has opposite signs at the two hot spots connected by the vector  $Q$ :

$$(\rho + Q) = -(\rho): \quad (1)$$

Thus, the eight hot spots can be divided into four groups (1,6), (2,5), (3,8), and (4,7), with the signs of  $\rho$  being opposite within each group. However, the relative signs of  $\rho$  between the different groups have to be determined from additional considerations.

In Fig. 1, the dashed and solid lines show the Fermi surfaces corresponding to the hole- and electron-doped cuprates. Notice that the point  $(0;0)$  is located at the corner of Fig. 1, so that the area inside the Fermi surface is occupied by holes and outside by electrons. The dashed Fermi surface, corresponding to the hole-doped

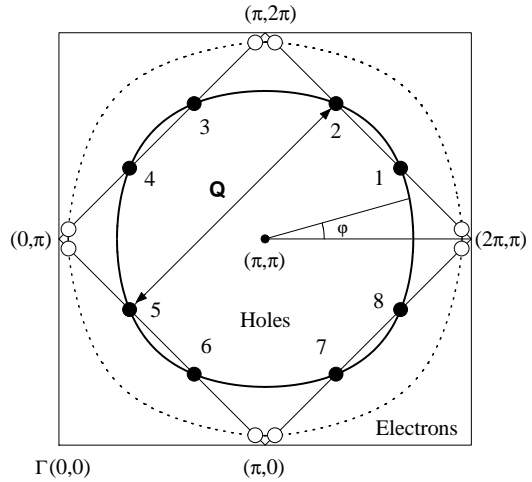


FIG. 1: Fermi surfaces of Eq. (2) for hole doping (dashed line,  $x = 0.176$ ,  $x = 0.15$ ) and electron doping (solid line,  $x = 0.15$ ,  $x = 0.176$ ). The hot spots are shown by open and solid circles. The radius of the circles  $= 0.1$  represents the width of the interaction (4) in the momentum space.

case, encloses a larger area, and the pairs of hot spots shown by the open circles in Fig. 1 are located close to the van Hove points  $(0;0)$ ,  $(\pi;0)$ ,  $(2\pi;\pi)$ , and  $(\pi;2\pi)$ . It is natural to assume that  $\rho$  has the same sign within each pair of the neighboring hot spots. This assumption, in combination with Eq. (1), immediately results in the familiar  $d_{x^2-y^2}$  symmetry of the pairing potential.

However, the situation does change in the electron-doped case. With the increase of electron doping, the Fermi surface shrinks, and the hot spots move away from the van Hove points toward the Brillouin zone diagonals. The following pairs of the hot spots approach each other: (1,2), (3,4), (5,6), and (7,8). The  $d_{x^2-y^2}$  pairing potential has opposite signs within each pair and vanishes at the zone diagonals. Thus, in the electron-overdoped

cuprates, when the hot spots get close enough, the  $d_{x^2-y^2}$  pairing becomes suppressed. Then, a superconducting pairing of another symmetry may emerge, with the pairing potential of the same sign on both sides of the zone diagonals. This is the mechanism that we propose for the transition observed in Refs. [3, 4].

**Suppression of  $d$ -wave pairing.** To illustrate how the  $d_{x^2-y^2}$  pairing evolves with doping, we perform calculations employing the typical electron dispersion law

$$\langle p \rangle = 2t_0 (\cos p_x + \cos p_y) + 4t_1 \cos p_x \cos p_y \quad (2)$$

with  $t_1 = t_0 = 0.45$ . The chemical potential controls the hole concentration  $n$ , which is determined by the area  $S$  inside the Fermi surface in Fig. 1:  $n = 2S = (2)^2$ . The doping  $x = n - 1$  is defined as the deviation of  $n$  from half

filling, so that  $x > 0$  and  $x < 0$  correspond to hole and electron doping [6]. The relation  $S / (1+x)$  is in agreement with the angular-resolved photoemission spectroscopy (ARPES), except for the region of small doping around  $x = 0$ , where the antiferromagnetic Mott insulating state intervenes. For  $\text{Nd}_{2-x}\text{Ce}_x\text{CuO}_4$ , this was established in Ref. [7], and movement of hot spots toward the zone diagonals with the increase of electron doping was directly observed in Refs. [7, 8, 9]. Notice that, for the dispersion law (2), the hot spots exist only within a finite range of chemical potential  $4t_1 > 0$ , which corresponds to the range of doping  $0.25 = x_- < x < x_+ = 0.53$ . The respective pairs of the hot spots merge and disappear at the van Hove points when  $x = x_-$  and at the zone diagonals when  $x = x_+$ . Thus, in this model, the  $d_{x^2-y^2}$  superconductivity can exist only within a finite range of electron and hole doping, in qualitative agreement with the experimental phase diagram of cuprates.

To verify the qualitative picture given in the Introduction, we solve the BCS equation for the pairing potential

$$\langle p \rangle = V(p - p^0) \frac{\tanh \frac{E(p^0)}{2T}}{2E(p^0)} - \langle p^0 \rangle \frac{d^2 p^0}{(2)^2} : \quad (3)$$

Here  $E(p) = \sqrt{p^2 + p^2}$ ,  $T$  is temperature, and  $V(q) = V_c(q) + V_s(q)$  is the effective interaction between electron charges and spins, where  $V_c$  and  $V_s$  are the Pauli matrices, and  $\langle \cdot \rangle$  are the spin indices. For singlet and triplet pairings, the functions  $V_0(q) = V_c(q) - 3V_s(q)$  and  $V_1(q) = V_c(q) + V_s(q)$  enter Eq. (3), respectively. To simplify our calculations, we ignore the frequency dependence of  $V$  and use the conventional AF interaction of the form

$$V_0(q) = \frac{g}{(q - Q)^2 + \omega^2} \quad (4)$$

with the coupling constant  $g = 2t_0$  and the width  $Q = 0.1$  [10].

The  $d_{x^2-y^2}$  pairing potential, calculated at  $T = 0$  for three different dopings, is shown in the main panel of

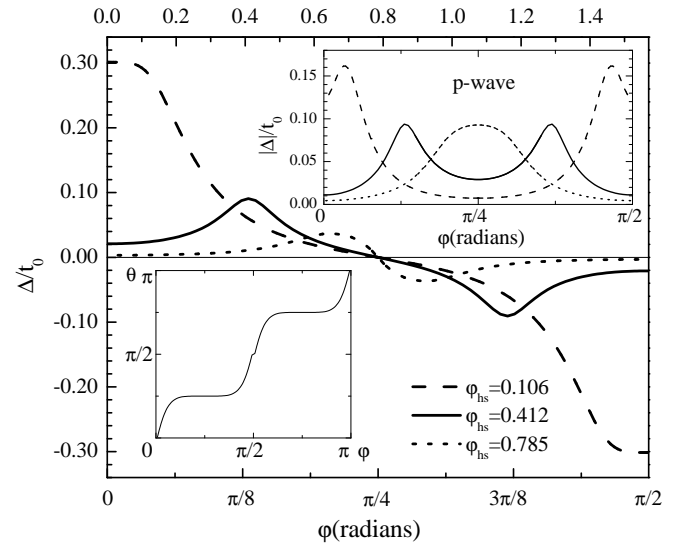


FIG. 2: The pairing potential at  $T = 0$  vs. the angle ' on the Fermi surface, shown by the dashed line for  $x = 0.37$  ( $= 1.6t_0$ ), the solid line for  $x = 0.1$  ( $= 0.6t_0$ ), and the dotted line for  $x = 0.25$  ( $= 0$ ). The main panel represents the  $d_{x^2-y^2}$  state, and the upper inset the chiral  $p$ -wave state. The angle '  $_{hs}$  indicates the position of the hot spot 1. The lower inset shows the phase of  $\Delta = j \phi$  for the chiral  $p$ -wave pairing.

Fig. 2 vs. the angle ' on the Fermi surface (see Fig. 1). The dashed line refers to the strong hole doping  $x = 0.37$  close to  $x_+$ , the dotted line to the strong electron doping  $x = 0.25$ , and the solid line to the intermediate electron doping  $x = 0.1$ . The angle '  $_{hs}$  indicates the position of the hot spot 1 for these dopings. We see that the maxima of  $j \Delta$  are achieved at the hot spots, i.e. at '  $_{hs}$ , as discussed in Ref. [11]. The solid curve in Fig. 2 qualitatively agrees with the nonmonotonic function ' inferred from the Raman scattering in  $\text{Nd}_{1.85}\text{Ce}_{0.15}\text{CuO}_4$  [12]. We also observe that  $j \Delta$  drops precipitously when the hot spots approach the zone diagonals. This happens because the integral in Eq. (3) is suppressed when positive and negative peaks of ' are close to each other.

**Alternative superconducting pairings.** Once the  $d_{x^2-y^2}$  pairing is suppressed in the case of strong electron doping, pairing of a different symmetry may emerge in the system. Evidently, this pairing should provide the same sign of ' within each pair (1,2), (3,4), (5,6), and (7,8) of the approaching hot spots. There are three possibilities depending on the relative signs of ' between the different pairs of the hot spots. The same sign for all the hot spots corresponds to s-wave, the opposite sign between (1,2) and (3,4) to  $d_{xy}$ -wave, and the opposite sign between (1,2) and (5,6) to triplet  $p$ -wave pairing.

Which of these states wins? The simplest assumption is that the s-wave pairing does, because it can be pro-

duced by phonons. In this case, the energy gap  $j$  has no nodes and is roughly uniform along the Fermi surface. This scenario is supported by the measurement of the temperature dependence of the penetration depth

(T) [4], which shows a transition from a gap with the nodes to a nodeless gap with the increase of electron doping in  $P_{2-x}Ce_xCuO_4$  and  $La_{2-x}Ce_xCuO_4$ . The point contact spectroscopy of  $P_{2-x}Ce_xCuO_4$  [3] shows a transition from a strong zero-bias conductance peak, originating from the midgap Andreev surface states in the d-wave case, to double peaks typical for s-wave. These experiments eliminate  $d_{xy}$ -wave as a possible successor to  $d_{x^2-y^2}$  in the electron-overdoped phase, because  $d_{xy}$  pairing has gap nodes and the midgap Andreev states. However, the s-wave scenario encounters some problems. When  $j$  ( $p$ ) varies along the Fermi surface, the measurement of (T) yields the minimal value of the gap  $\Delta_{min}$  at  $T = 0$ . The experiment [13] found  $\Delta_{min}/T_c \approx 0.85$ , whereas, for the phonon-induced s-wave superconductivity, this ratio should be close to the BCS value 1.76. Furthermore, for the phonon mechanism,  $T_c$  is not expected to depend on doping significantly, whereas the experimental  $T_c$  declines steeply at  $|x| > 0.15$  and vanishes for  $|x| > 0.2$  outside of the dome-shaped phase diagram of the electron-doped cuprates [14]. Incidentally, the value of doping where superconductivity disappears is close to  $x_c$ , which indicates that the hot spots may be equally important for the alternative superconducting pairing.

Thus, it is worth considering the last alternative pairing, namely the triplet p-wave. It has the order parameter  $n$ , where  $n$  is the antisymmetric metric tensor, and  $n$  is the unit vector of spin-polarization [23]. The symmetry of triplet pairing in a tetragonal crystal was classified in Ref. [15]. In the  $E_u$  representation,  $n$  points along the c axis, and the phase of  $(p)$  changes by  $2\pi$  around the Fermi surface. This order parameter is chiral and breaks the time-reversal symmetry. The simplest example is  $(p) / (\sin p_x + i \sin p_y)$ , which was originally proposed for  $Sr_2RuO_4$  [16]. In the  $A_{1u}$ ,  $A_{2u}$ ,  $B_{1u}$ , and  $B_{2u}$  representations, the vector  $n$  lies in the (a;b) plane and rotates around the Fermi surface by the angle  $2\pi$ . These order parameters are not chiral and do not break the time-reversal symmetry. The both types of the pairing potential have two components ( $j_1$ ;  $j_2$ ), the real and imaginary parts of  $n$  in the chiral case and  $(n_x; n_y)$  in the nonchiral case, which satisfy the symmetry relation  $j_2(p_x; p_y) = j_1(p_y; p_x)j$ . Then, the gap  $j = \sqrt{j_1^2 + j_2^2}$  does not have nodes, but is modulated along the Fermi surface. This easily explains the reduced value of  $\Delta_{min}/T_c$  observed in Ref. [13]. The tunneling spectrum, shown in Fig. 3 of Ref. [17] for  $(p) / (\sin p_x + i \sin p_y)$ , has double peaks, as in the experiment [3]. Thus, the existing experiments are not sufficient to distinguish between s- and p-wave pairings. It is desirable to measure the Knight shift below  $T_c$  in the electron-overdoped cuprates. If it does not change from

the normal state, that would be an indication of triplet pairing, like in  $Sr_2RuO_4$  [18] and the organic superconductors  $(TMFSF)_2X$  [19]. The time-reversal symmetry breaking can be detected by the muon spin-relaxation measurements, as in  $Sr_2RuO_4$  [20], or by measuring the local magnetic field produced by the chiral Andreev surface states. Quantitative estimates done in Ref. [21] show that the latter effect can be realistically observed with a scanning SQUID microscope [22].

Competition between d- and p-wave pairings. Since the ASF interaction has unfavorable sign for p-wave pairing, a different mediator is needed. Triplet pairing is usually associated with the ferromagnetic spin fluctuations (FSF), e.g. in the superfluid He-3 [23] or  $Sr_2RuO_4$  [24]. But we focus our attention on another possible mediator for p-wave pairing, namely the charge density fluctuations (CDF) enhanced in the vicinity of the charge-density-wave (CDW) instability. The latter is known to occur in the two-dimensional helium model at the relevant electron densities [25]. In a crystal, the CDW wave vector is expected to be close to  $Q = (1/2, 1/2)$ , and the CDF interaction  $V_c(q)$  would have a peak at this vector. This interaction has repulsive sign in the singlet and triplet particle-particle channels, resulting in the condition (1) and supporting both d- and p-wave superconducting pairings. The relative strength of CDF vs. ASF in cuprates is subject to debate. On one hand, neutron scattering observes the antiferromagnetic order in  $Nd_{1.85}Ce_{0.15}CuO_4$  [26]. On the other hand, measurements in heterostructure junctions show no mixing of antiferromagnetism and superconductivity [27].

Detailed evaluation of  $V_c(q)$  is not the purpose of our paper [10]. Instead, we employ a toy model with the same interaction in the triplet and singlet channels:  $V_1(q) = V_0(q) = V_c(q)$ , where  $V_c(q)$  is given by Eq. (4). Then, the difference in the solutions of the BCS equation (3) for d- and p-wave pairings results only from the geometry of the Fermi surface. The upper inset in Fig. 2 shows the magnitude  $j(|\mathbf{q}|)$  and the lower inset the phase of  $j(|\mathbf{q}|) = j_1 e^{i\phi_1}$  calculated for the chiral p-wave pairing. We observe that  $j(|\mathbf{q}|)$  has maxima at the hot spots angles  $\theta_{hs}$ , but, unlike in the  $d_{x^2-y^2}$  case, it does not vanish at  $\theta_{hs} = \pi/4$  and is not suppressed when the hot spots approach the zone diagonals. Fig. 2 is qualitatively consistent with the ARPES measurements [9] of  $j(|\mathbf{q}|)$ .

In Fig. 3, we show how various quantities depend on doping  $x$ . Panel (a) shows the hot spot angle  $\theta_{hs}$ . Panels (b), (c), and (d) show the transition temperature  $T_c$ , the maximal gap  $\Delta_{max}$ , and the condensation energy  $F$  for the  $d_{x^2-y^2}$  and chiral p-wave pairings. It is clear from Fig. 3 that, at the doping around  $x \approx 0.1$ , where the hot spots approach close enough to the zone diagonals, p-wave pairing wins over  $d_{x^2-y^2}$  pairing. The transition is of the first order as a function of  $x$  and has nothing to do with the quantum critical point [28]. With further increase of electron doping beyond  $x_c$ , hot spots disappear,

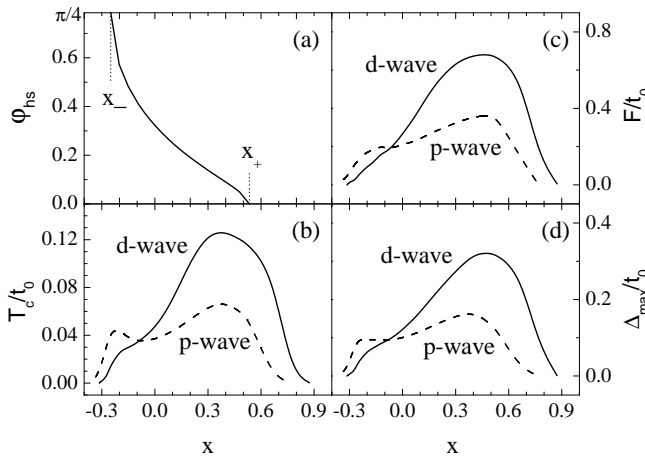


FIG. 3: Dependence of various quantities on doping  $x$ . Panel (a): the hot spot angle  $\Phi_{hs}$ , panel (b): the transition temperature  $T_c$ , panel (c): the condensation energy  $F$ , and panel (d): the maximum gap  $\Delta_{max}$ . The solid and dashed lines correspond to the  $d_{x^2-y^2}$  and p-wave pairings.

and the proposed p-wave superconductivity rapidly vanishes, in agreement with the experimental phase diagram [14]. It would be very interesting to obtain the superconducting phase diagram in the electron-overdoped regime simultaneously with the ARPES measurements of the hot spots positions. This kind of study was performed for the hole-doped  $\text{La}_{2-x}\text{Sr}_x\text{CuO}_4$  in Ref. [29]. Comparing Figs. 7 and 8 of Ref. [29], one can see that d-wave superconductivity vanishes in the hole-overdoped regime  $x > x_+$ , where the hot spots merge at the van Hove points and disappear, in qualitative agreement with our arguments and Fig. 3.

**Conclusions.** We have shown that, when the hot spots approach the Brillouin zone diagonals in the electron-overdoped cuprates,  $d_{x^2-y^2}$  pairing becomes unfavorable and is replaced by either singlet s-wave or triplet p-wave. The transition is of the first order as a function of doping  $x$ . We have given a number of arguments in favor of the triplet p-wave pairing, which may break the time-reversal symmetry. To verify the proposed scenario, it is desirable to measure correlation between  $T_c$  and the hot spots positions by ARPES. The Knight shift measurements can test the triplet character of pairing, while the muon spin-relaxation and the scanning SQUID experiments can detect spontaneous violation of the time-reversal symmetry.

VAK and VMY thank R.L. Greene for useful discussions, and the Kavli Institute for Theoretical Physics for the opportunity to start this collaboration. VAK thanks the Condensed Matter Theory Center for arranging his visit to the University of Maryland. VMY is supported by the NSF Grant DMR-0137726, HY by the scholarship from Ewha Womans University and by Korean Research

Foundation, VAK by the NSF Grant PHY-0140316 and by the McDonnell Center for Space Sciences, and VAK and MVZ by the Grant 00-15-96590 from the Russian Foundation for Basic Research and Grant NSh-1885.2003.2 from the Russian Ministry of Industry and Science.

- [1] D. H. Wu et al., *Phys. Rev. Lett.* **70**, 85 (1993).
- [2] C. C. Tsuei and J. R. Kirtley, *Phys. Rev. Lett.* **85**, 182 (2000); J. D. Kokalj et al., *ibid.* **85**, 3696 (2000); R. Prozorov et al., *ibid.* **85**, 3700 (2000).
- [3] A. Biswas et al., *Phys. Rev. Lett.* **88**, 207004 (2002).
- [4] J. A. Skinta et al., *Phys. Rev. Lett.* **88**, 207005 (2002).
- [5] D. J. Scalapino, *Phys. Repts.* **250**, 329 (1995); D. Pines, *Physica B* **163**, 78 (1990); T. Morigami, Y. Takahashi, and K. Ueda, *J. Phys. Soc. Jpn.* **59**, 2905 (1990).
- [6] This definition of  $x$  is consistent with the doping parameter  $x$  in the chemical formulas, such as  $\text{La}_{2-x}\text{Sr}_x\text{CuO}_4$ .
- [7] N. P. Amritage et al., *Phys. Rev. Lett.* **88**, 257001 (2002).
- [8] N. P. Amritage et al., *Phys. Rev. Lett.* **87**, 147003 (2001).
- [9] N. P. Amritage et al., *Phys. Rev. Lett.* **86**, 1126 (2001).
- [10] The purpose of our calculations is not to achieve precise numerical agreement with the experiment, but rather to illustrate how the proposed mechanism works within a simple model. The parameters of the model are not optimized for any particular material, and we neglect their dependence on  $x$ .
- [11] V. A. Khodel and V. M. Yakovenko, *Phys. ZhETF* **77**, 494 (2003) [*JETP Lett.* **77**, 420 (2003)].
- [12] G. Blumberg et al., *Phys. Rev. Lett.* **88**, 107002 (2002).
- [13] J. A. Skinta et al., *Phys. Rev. Lett.* **88**, 207003 (2002).
- [14] J. L. Peng et al., *Phys. Rev. B* **55**, R 6145 (1997); A. Sawada et al., *ibid.* **66**, 014531 (2002); H. Takagi, S. Uchida, and Y. Tokura, *Phys. Rev. Lett.* **62**, 1197 (1989).
- [15] G. E. Volovik and L. P. Gor'kov, *Zh. Eksp. Teor. Fiz.* **88**, 1412 (1985) [*Sov. Phys. JETP* **61**, 843 (1985)]; M. Sigrist and K. Ueda, *Rev. Mod. Phys.* **63**, 239 (1991).
- [16] K. Miyake and O. Narikiyo, *Phys. Rev. Lett.* **83**, 1423 (1999).
- [17] K. Sengupta, H.-J. Kwon, and V. M. Yakovenko, *Phys. Rev. B* **65**, 104504 (2002).
- [18] K. Ishida et al., *Nature* **396**, 658 (1998).
- [19] I. J. Lee et al., *Phys. Rev. Lett.* **88**, 017004 (2002).
- [20] G. M. Luke et al., *Nature* **394**, 558 (1998).
- [21] H.-J. Kwon, V. M. Yakovenko, and K. Sengupta, *Synthetic Metals* **133-134**, 27 (2003).
- [22] R. C. Black et al., *Appl. Phys. Lett.* **62**, 2128 (1993); L. N. Vu et al., *Appl. Phys. Lett.* **63**, 1693 (1993); C. C. Tsuei et al., *Phys. Rev. Lett.* **73**, 593 (1994); K. A. Moler et al., *Science* **279**, 1193 (1998).
- [23] D. Vollhardt and P. W.ole, *The Superuid Phases of Helium 3* (Taylor and Francis, London, 1990).
- [24] I. I. Mazin and D. J. Singh, *Phys. Rev. Lett.* **79**, 733 (1997); **82**, 4324 (1999).
- [25] L. Swierkowski, D. Neilon, and J. Szymanski, *Phys. Rev. Lett.* **67**, 240 (1991); A. Gold and L. Calmels, *Phys. Rev. B* **48**, 11622 (1993).
- [26] H. J. Kang et al., *Nature* **423**, 522 (2003).
- [27] I. Bozovic et al., *Nature* **422**, 873 (2003).
- [28] M. Vojta, Y. Zhang, and S. Sachdev, *Phys. Rev. Lett.* **85**, 4940 (2000).
- [29] A. Ino et al., *Phys. Rev. B* **65**, 094504 (2002).